PCP
PLANT & CELL PHYSIOLOGY

From Organelle to Organ: ZRIZI MATE-Type Transporter is an Organelle Transporter that Enhances Organ Initiation

Yogev Burko[1], Yosef Geva[1], Aya Refael-Cohen[1], Sharona Shleizer-Burko[1], Eilon Shani[1], Yael Berger[1], Eyal Halon[1], George Chuck[2], Menachem Moshelion[1,*] and Naomi Ori[1,*]

[1]The Robert H. Smith Institute of Plant Sciences and Genetics in Agriculture and The Otto Warburg Minerva Center for Agricultural Biotechnology, Hebrew University, Rehovot 76100, Israel

[2]Plant Gene Expression Center, 800 Buchanan St., Albany, CA 94710, USA

*Corresponding authors: Naomi Ori, E-mail, ori@agri.huji.ac.il; Fax, +972-8-948-9322; Menachem Moshelion, E-mail, moshelio@agri.huji.ac.il; Fax, +972-8-948-9781

(Received November 19, 2010; Accepted January 11, 2011)

Regular Paper

Plant architecture is a predictable but flexible trait. The timing and position of organ initiation from the shoot apical meristem (SAM) contribute to the final plant form. While much progress has been made recently in understanding how the site of leaf initiation is determined, the mechanism underlying the temporal interval between leaf primordia is still largely unknown. The Arabidopsis *ZRIZI* (*ZRZ*) gene belongs to a large gene family encoding multidrug and toxic compound extrusion (MATE) transporters. Unique among plant MATE transporters identified so far, ZRZ is localized to the membrane of a small organelle, possibly the mitochondria. Plants overexpressing *ZRZ* in initiating leaves are short, produce leaves much faster than wild-type plants and show enhanced growth of axillary buds. These results suggest that ZRZ is involved in communicating a leaf-borne signal that determines the rate of organ initiation.

Keywords: Arabidopsis • Architecture • Enhancer trap • MATE transporters • Organ initiation rate • ZF14.

Abbreviations: GFP, green fluorescent protein; GUS, β-glucuronidase; MATE, multidrug and toxic compound extrusion; OP, operator; qRT–PCR, quantitative reverse transcription0–PCR; SAM, shoot apical meristem.

Introduction

The plant body is formed through a series of morphogenetic events, coordinated by meristems. The shoot apical meristem (SAM) continuously produces lateral organs, axillary meristems and stems, successively building the plant shoot (Bowman and Eshed 2000, Carles and Fletcher 2003, Veit 2006, Barton 2010). While the outcome of this sequence of events is unique in every single plant (Sachs 2004), reflecting the changing internal and external circumstances, many features of plant architecture are highly predictable within a given species. Thus, organ formation and growth at the SAM are tightly regulated in a manner that enables this combination of consistency and flexibility.

The time period between the initiation of two successive leaves is termed the plastochron. The timing of leaf initiation is thought to be determined by non-autonomous signals from the previously initiated leaf (Lee et al. 2009). The timing of organ initiation from the SAM, the extent of stem growth between initiated organs and the fate of the axillary meristems represent central developmental choices affecting plant architecture (Reinhardt and Kuhlemeier 2002, McSteen and Leyser 2005). Mutant analysis suggests that these features, as well as leaf size, may be related, as they are often commonly affected by a single genetic lesion (Schwarz et al. 2008, Wang et al. 2008).

The Arabidopsis *altered meristem program1* (*amp1*) mutant, which is allelic to *primordia timing* (*pt*), *hauptling* (*hpt*) and *constitutive morphogenesis 2* (*cop2*), shows an increased rate of leaf initiation, shorter internodes, reduced apical dominance, de-etiolation in the dark and earlier flowering time (Chaudhury et al. 1993, Hou et al. 1993, Conway and Poethig 1997, Mordhorst et al. 1998). The *AMP1* gene encodes a putative glutamate carboxypeptidase, and has been implicated in the production of a signaling molecule involved in SAM function (Helliwell et al. 2001). *amp1* mutants contain increased cytokinin levels, and many aspects of its altered phenotype are also associated with exogenous cytokinin application (Chaudhury et al. 1993). However, some of the *amp1* effects cannot be phenocopied by cytokinin application. This, and the nature of the *AMP1* gene, suggests that the elevated cytokinin level may not be the primary effect of the mutation, and that additional, cytokinin-independent processes may be impaired in *amp1* mutants (Helliwell et al. 2001, Saibo et al. 2006).

Mutations in the *SUPERSHOOT* (*SPS*) gene, encoding a cytochrome P450, also cause a dramatic increase in cytokinin levels. *sps* mutants are characterized by an extreme overgrowth of axillary shoots, which may be mediated by the increased cytokinin levels (Tantikanjana et al. 2001). The phenotypes of *sps* and *amp1* mutants only partially overlap despite the common

Plant Cell Physiol. 52(3): 518–527 (2011) doi:10.1093/pcp/pcr007, available online at www.pcp.oxfordjournals.org

feature of elevated cytokinin levels, suggesting that relative spatial and temporal cytokinin levels play a crucial role in these phenotypes.

The *miR156*-regulated transcription factors SPL9 and SPL15 have been shown to regulate leaf initiation rate and branching redundantly. Reduced activity of SPL9 and SPL15 resulted in an increased leaf initiation rate, suggesting that these factors negatively affect leaf initiation (Schwarz et al. 2008, Wang et al. 2008). Double mutants in *CYP78A5/KLUH* and its close homolog *CYP78A7* also cause an increased leaf initiation rate, probably in a pathway parallel to that of SPL (Anastasiou et al. 2007, Wang et al. 2008). An increased rate of leaf initiation has also been observed in the maize *terminal ear1* (*te1*) and the rice *plastochron1* (*pla1*) and *pla2* mutants. *te1* and *pla2* represent mutations in orthologous genes encoding RNA-binding proteins (Veit et al. 1998, Kawakatsu et al. 2006). While *TE1* is expressed in both the maize SAM and leaf primordia, the *PLA2* gene is expressed mostly in leaf primordia. The *PLA1* gene encodes the cytochrome P450 CYP78A11, and is expressed in specific regions of developing leaves (Miyoshi et al. 2004). Thus, control of the rate of leaf initiation seems to involve diverse biochemical activities and complex communication between the initiating leaf and the SAM. Moreover, it appears that many of the players involved in this delicately balanced process are not yet known.

Multidrug and toxic compound extrusion (MATE) is a family of transporter proteins, which is widely distributed in all living kingdoms (Brown et al. 1999, Omote et al. 2006). The plant *MATE* gene family is particularly large, with 58 members in the Arabidopsis genome (Hvorup et al. 2003, Omote et al. 2006). However, the biological function of most of its family members is still unknown. Plant MATE proteins are reported to be localized to the tonoplast or the plasma membrane, and to transport secondary metabolites and xenobiotics through an H^+ exchange mechanism. They are implicated in various processes, including anthocyanin accumulation (Debeaujon et al. 2001, Mathews et al. 2003, Marinova et al. 2007, Gomez et al. 2009, Zhao and Dixon 2009), protection of roots from inhibitory compounds (Diener et al. 2001), salicylic acid-dependent disease resistance signaling (Nawrath et al. 2002), iron homeostasis (Rogers and Guerinot 2002, Durrett et al. 2007), aluminum tolerance (Magalhaes et al. 2007, Liu et al. 2009, Maron et al. 2010) and detoxification of lipophilic cations and cadmium (Li et al. 2002). To date, MATE proteins have not been implicated in plant development.

Here, we describe the characterization of a member of the Arabidopsis MATE gene family, *ZRIZI* (*ZRZ*; 'ZARIZ' means agile in Hebrew). *ZRZ* overexpression in initiating leaves resulted in short, bushy plants with a dramatically increased leaf initiation rate. Intracellular localization analysis revealed that ZRZ is located in the membrane of mitochondria, or an organelle that is biochemically related to mitochondria. The ZRZ transporter is thus proposed to be involved in the determination of the leaf initiation rate through an unknown mechanism.

Results

ZRIZI—a MATE gene with enriched expression in shoot apices

A screen of enhancer trap lines has identified a line, designated 1015, with enriched expression in the boundaries between the developing leaf primordia and the developing stem (**Supplementary Fig. S1A-C**). In the inflorescence, strong staining was observed in the receptacles, in addition to the inflorescence meristem (**Supplementary Fig. S1D**).

The insertion site in 1015 was located on chromosome 1, about 5 kb upstream of the annotated gene *At1g58340* (*ZF14*; Kato et al. 1999), and about 7 kb downstream from *At1g58330* (*ZW2*) (**Fig. 1A**). Examination of *ZF14* transcript levels in Arabidopsis shoots using quantitative reverse transcription–PCR (qRT–PCR) revealed that its expression is enriched in shoot apices relative to leaves, in agreement with the 1015 expression pattern (**Fig. 1B–E**). In contrast, ZW2 is expressed ubiquitously in the plant, as revealed by the Arabidopsis eFP browser (http://bbc.botany.utoronto.ca/efp/cgi-bin/efpWeb.cgi) (Winter et al. 2007), and is transcribed in the opposite direction with respect to the insertion. We chose to characterize further the *ZF14* (*At1g58340*) gene, referred to below as *ZRZ*. *ZRZ* encodes a protein from the MATE family of multidrug-transporter proteins.

Subcellular localization of ZRZ

To follow ZRZ cellular localization, we transiently expressed a chimeric green fluorescent protein (GFP)–ZRZ fusion protein under the control of two copies of the 35S promoter in protoplasts from Arabidopsis mesophyll. GFP–ZRZ expression was localized to organelles (**Fig. 2A, B**) with a similar distribution profile and number to those of the mitochondria (detected using the mitochondrion-selective red dye MitoTracker; **Fig. 2C**). However, GFP–ZRZ and MitoTracker did not co-localize to the same organelle (**Fig. 2D**; see also **Supplementary Fig. S2**). Interestingly, in cells strongly expressing GFP–ZRZ the mitochondria showed weaker labeling with MitoTracker (**Supplementary Fig. S2**). This weaker labeling was specifically related to ZRZ expression, as the control, which expressed free GFP, did not show such an effect (**Supplementary Fig. S2**). These results indicate the existence of a direct or indirect relationship between ZRZ and mitochondrial activity.

ZRZ misexpression causes dramatic developmental phenotypes

To examine ZRZ function, we characterized mutant lines with insertions in the *ZRZ* gene. *zrz-1* mutants, homozygote for an insertion in the first exon of *ZRZ*, about 100 bp downstream from the start codon (**Fig. 1A**), did not show any aberrant phenotype compared with the wild type (**Supplementary Fig. S3A, B**). qRT–PCR analysis showed 83-fold lower *ZRZ* mRNA levels in *zrz-1* seedlings (**Supplementary Fig. S3C**).

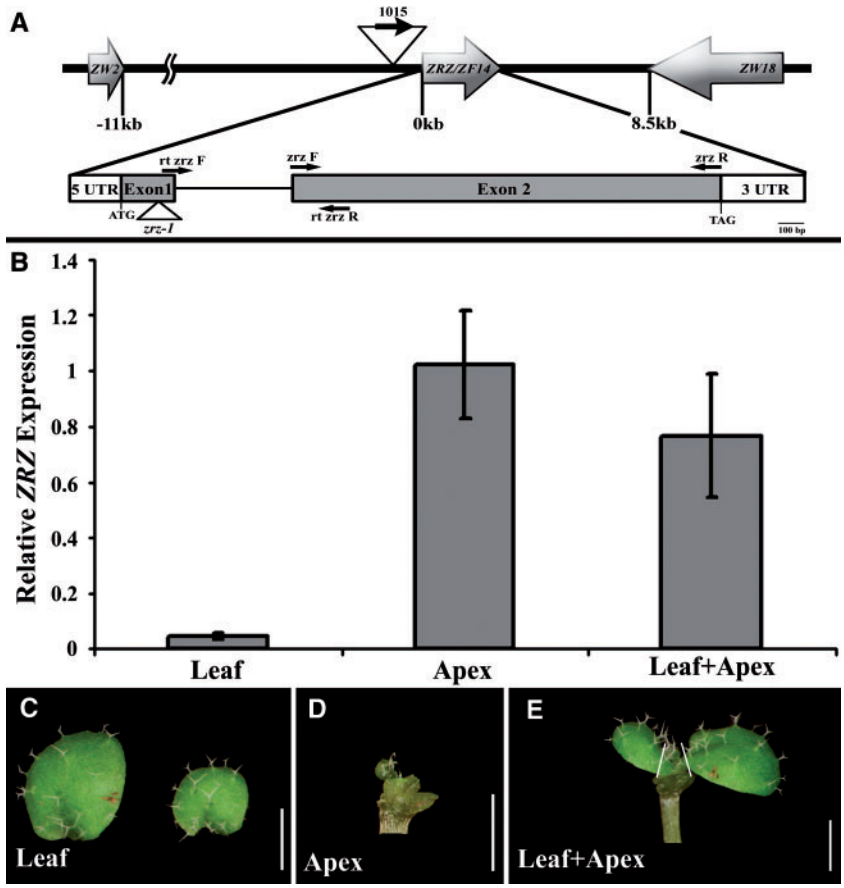

Fig. 1 The *ZRIZI* (*ZRZ/ZF14*) gene structure and its expression in different tissues. (A) Scheme of the genomic location of *ZRZ* (top) and the *ZRZ* gene structure (bottom). Wide arrows and solid black lines represent annotated genes and intergenic regions, respectively. The insertion sites in the 1015 enhancer trap line and in *zrz-1* are indicated by triangles. Exons, introns, the untranslated region (UTR), start and stop codons are indicated. Primers used in this study are indicated with black arrows. (B) Levels of *ZRZ* mRNA from 20-day-old seedlings were assayed by qRT–PCR relative to the *TUB* internal control, and are shown as an average of three biological repeats (±SE) for the indicated tissues. (C–E) The tissues from which the samples in (B) were collected are shown. Scale bars = 1 mm.

The lack of apparent phenotype in *zrz-1* mutants may result from redundant activity of additional MATE genes. Therefore, to understand ZRZ function further, we misexpressed the gene by the use of several different promoters. *ZRZ* expression driven by the *35S* promoter resulted in tiny, bushy and almost infertile plants (**Fig. 3A–F**).

We used a transactivation system (Moore et al. 1998) to analyze further the specific effect of *ZRZ* misexpression in different domains. The *AINTEGUMENTA* (*ANT*) promoter is expressed in lateral organ primordia from a very early stage (Elliott et al. 1996, Schoof et al. 2000). *ZRZ* expression driven by the *ANT* promoter resulted in similar phenotypes to those of *35S:ZRZ* plants (**Fig. 4A–H, L**; compare with **Fig. 3A–F**). However, the phenotypes were milder and the plants were partially fertile.

ANT>>ZRZ plants produced leaves much faster than wild-type plants (**Figs. 4A, B**, **5A**). While in 14-day-old wild-type plants an average of 6.4 (±0.5) leaves were produced, *ANT>>ZRZ* plants of comparable age produced 9.6 (±0.8) leaves (**Fig. 5A**). Similarly, 16-day-old wild-type and *ANT>>ZRZ* plants had 8 (± 0.67) and 11.81 (±0.74) leaves, respectively. While *ANT>>ZRZ* plants flowered early with respect to chronological age, they produced 11.81 (±0.74) leaves before flowering, relative to 8.4 (±0.84) leaves in the wild type. Similarly, upon flowering, *ANT>>ZRZ* plants produced flowers faster than the wild type (**Fig. 5B**). In addition, they featured reduced stem elongation and altered phylotaxis (**Figs. 4E, G, H, K, L**, **5C**). A role for ZRZ in the control of leaf initiation rate is in agreement with the enriched expression of *ZRZ* in young apices relative to older leaves (**Fig. 1B**).

The bushy appearance of *ANT>>ZRZ* plants resulted from the combination of reduced stem elongation and reduced apical dominance. More rosette leaves developed a visible axillary bud in *ANT>>ZRZ* than in wild-type plants (**Fig. 4C, D**). To quantify this phenotype, the proportion of individuals producing a visible axillary bud in the axil of each leaf was recorded. As can be seen in **Fig. 5E**, 44% of *ANT>>ZRZ* plants produced axillary buds in the axil of the cotyledon, while in wild-type

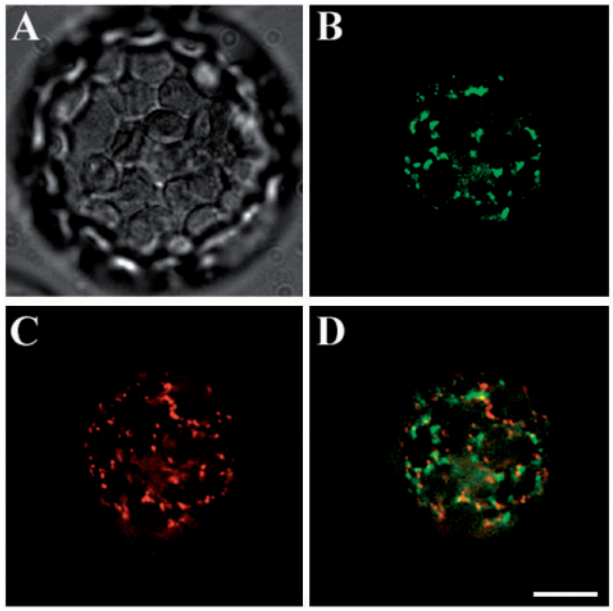

Fig. 2 ZRZ subcellular localization in protoplasts. Epifluorescent images of the GFP–ZRZ fusion protein, transiently expressed in Arabidopsis mesophyll protoplasts loaded with a mitochondrion-selective dye. (A) Bright field image of the protoplast cytoplasm. (B and C) Epifluorescent images of the same protoplast as in A, showing the localization of the GFP–ZRZ fusion protein in green (B, excitation 488 nm; emission 520 nm) and the MitoTracker in red (C, excitation 579 nm; emission 599 nm); the GFP–ZRZ fusion protein is localized to cytoplasmic organelles. (D) Superimposed images B and C reveal that the two fluorophore markers do not co-localize. Scale bars = 10 μm.

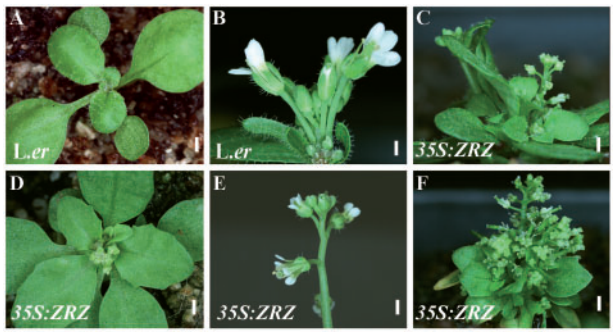

Fig. 3 *ZRZ* overexpression dramatically affects plant architecture. (A and D) Twenty-one-day-old seedlings. (B and E) Inflorescences. (C and F) Mature plants. L.*er*, wild type, *35S:ZRZ*, plants expressing *ZRZ* under the control of the 35S promoter. Scale bars = 1 mm.

plants buds were not observed in the cotyledon axil. A dramatic increase relative to the wild type was also observed in the number of plants producing a bud in the axil of additional early leaves (**Fig. 5E**). Also, more axillary buds had elongated in 15-day-old *ANT>>ZRZ* plants than in the wild type (**Fig. 5D**).

ANT>>ZRZ and *35S:ZRZ* plants produced organs with aberrant shape and smaller size. Leaves were smaller and more serrated than wild-type leaves (**Figs. 3A, D**, **4A, B**). Flowers were smaller than in the wild type (**Fig. 4G, H**), and siliques were shorter and aberrant (**Fig. 4F**). Flowers showed reduced fertility.

To confirm that the observed phenotypes were caused by overexpression of the *ZRZ* gene, levels of *ZRZ* mRNA were compared between whole seedlings of the wild type and *ANT>>ZRZ*. *ANT>>ZRZ* seedlings were found to have a dramatically elevated *ZRZ* mRNA level relative to the wild type (**Fig. 4N**).

To test the effect of the location of *ZRZ* expression on the phenotype, we expressed *ZRZ* with the *STM* promoter. The *STM* promoter drives expression in the SAM and not in leaf primordia, thus representing complementary expression to that of *ANT*. ZRZ expression driven by the *STM* promoter did not have an obvious effect during the vegetative phase of plant development, but after the transition to flowering these plants had similar phenotypes to those of *ANT>>ZRZ* (**Fig. 4I–M**). Thus, accurate *ZRZ* expression is critical for properly balanced organ production at the SAM. While *ZRZ* expression in leaf primordia dramatically affects leaf initiation rate and plant architecture, the SAM is relatively insensitive to ZRZ activity.

Levels of *CYP78A5/KLUH* mRNA, encoding a putative cytochrome P450 monooxygenase and expressed in a boundary region at the periphery of the SAM (Zondlo and Irish 1999), were dramatically elevated in the *amp1* mutant and its allele *pt1*, as well as following cytokinin treatment (Helliwell et al. 2001). However, double mutants in *CYP78A5/KLUH* and its close homolog *CYP78A7* also resulted in reduced plastochron length (Anastasiou et al. 2007, Wang et al. 2008). We compared *CYP78A5/KLUH* expression in *ANT>>ZRZ* and wild-type plants, to test whether common targets are affected in *ANT>>ZRZ* and *amp1/pt1*. *CYP78A5/KLUH1* mRNA levels were elevated in *ANT>>ZRZ* plants (**Fig. 6**). Thus, the *amp1* mutation and *ZRZ* overexpression appear to affect partially overlapping processes.

Discussion

While significant progress has been made recently in elucidation of the mechanisms underlying the decision as to when, where and how frequently organs are produced from the SAM, we are far from fully understanding the complex communication network that confers both consistency and flexibility to the timing of organ formation. We show that the specific site of ectopic expression of a MATE transporter, encoded by the *ZRZ* gene, dramatically affects the rate of organ production, as well as internode length and apical dominance. These findings reveal that members of this MATE protein family are involved in a much broader range of biological activities than previously suspected, including developmental processes.

Our results indicate that ZRZ is involved in specifying the lateral organ initiation rate. Enhanced *ZRZ* expression in the

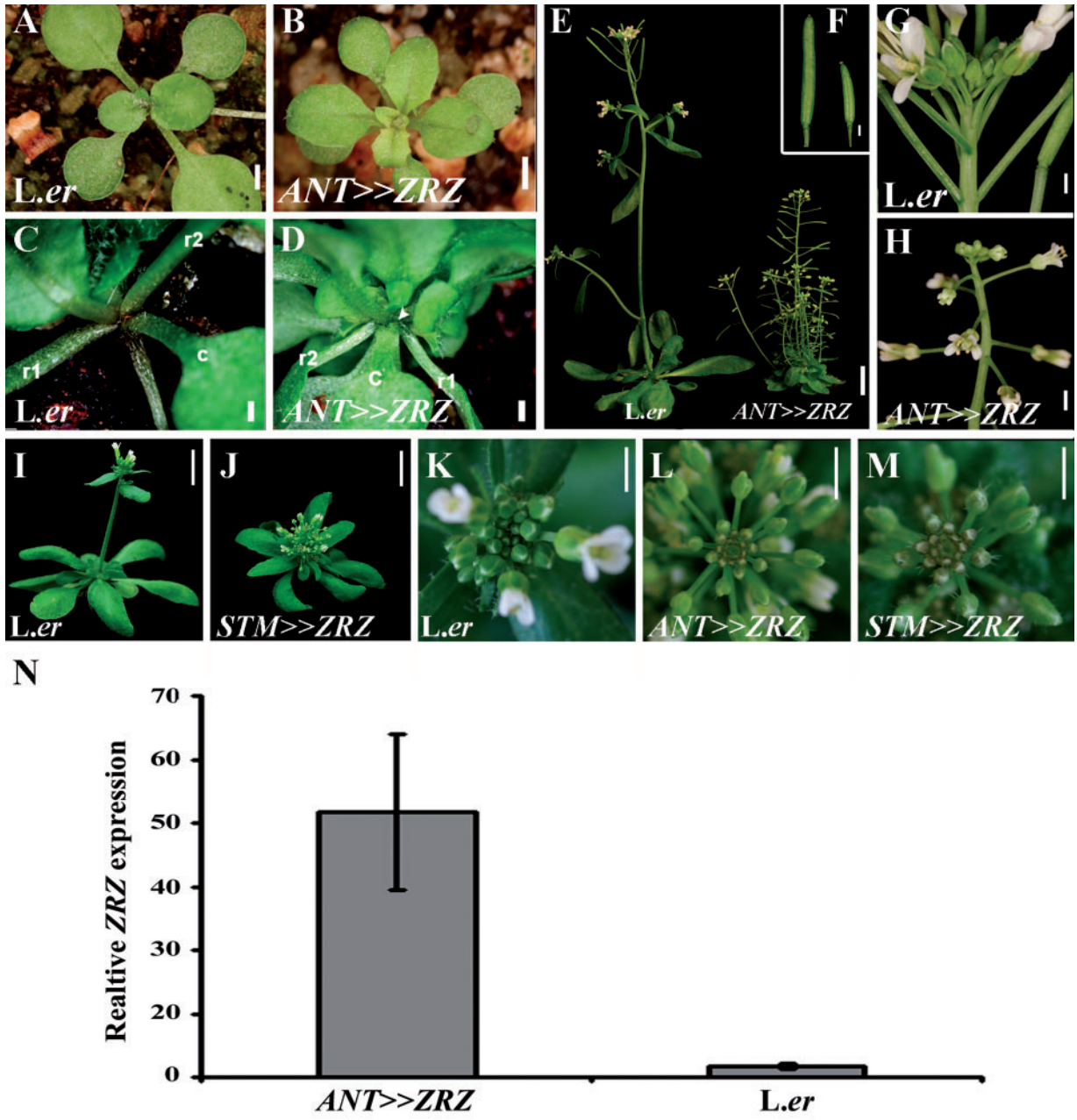

Fig. 4 *ZRZ* misexpression in specific tissues leads to altered plastochron and increased numbers of axillary branches. (A and B) Sixteen-day-old seedlings. (C and D) A closer view of the rosette leaves' axils, showing the abundance and premature growth of axillary meristems (arrow) in *ANT>>ZRZ* plants. (E) Mature plants. (F) Siliques of wild-type (left) and *ANT>>ZRZ* (right) plants. (G and H) Inflorescences. (I and J) Thirty-day-old plants. (K–M) Top view of the inflorescences of the indicated genotypes. In A–M, genotypes are indicated at the bottom left corner of each image. (N) *ZRZ* expression in 21-day-old plants, assayed by qRT–PCR. Averages (±SE, $n = 3$ biological repeats in *ANT>>ZRZ* and $n = 4$ in L*er*) of *ZRZ* levels, presented relative to the expression of the *TUB* internal control are shown for the indicated genotypes. L*er*, wild type control; *ANT>>ZRZ*, plants expressing *pANT:LhG4* and *OP:ZRZ*; c, cotyledon; r1, r2, first and second rosette leaves, respectively. Scale bars = A–H 1 mm, I M 2.5 mm.

primordia results in faster organ production. In contrast, its enhanced expression in the SAM driven by the *STM* promoter does not affect the organ initiation rate significantly during vegetative development. These findings indicate that the specific expression domain of ZRZ affects organ initiation rate, and that leaf primordia but not the SAM are responsive to enhanced ZRZ activity.

How might a MATE transporter affect the timing of organ initiation? The timing of leaf initiation is thought to be affected by an inhibitory signal from the developing leaf (Snow and

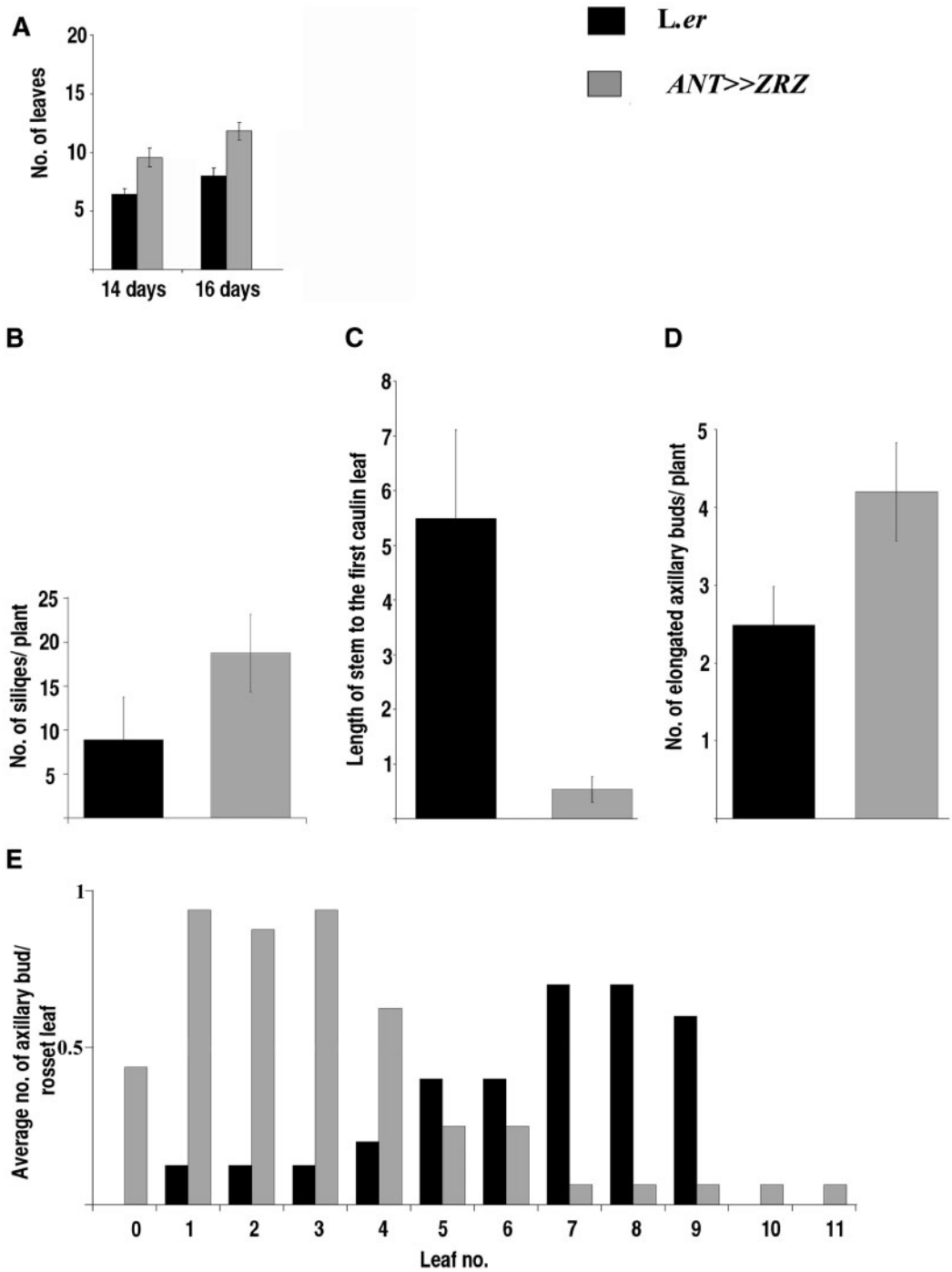

Fig. 5 Quantification of the *ANT>>ZRZ* phenotype. (A) Number of leaves produced by wild-type (L.*er*) and *ANT>>ZRZ* plants at the indicated ages. Shown are averages ± SD ($n = 10$ for L.*er* and $n = 16$ for *ANT>>ZRZ*). (B) Number of siliques. Siliques were counted on plants that ceased producing siliques. (C) Length of the first internode. (D) Total number of elongated axillary buds. In B–D, averages ± SD are shown ($n = 9$ for L.*er* and $n = 8$ for *ANT>>ZRZ*). (E) Number of axillary buds in the axils of the cotyledons and each rosette leaf ($n = 10$ in L.*er* and $n = 16$ in *ANT>>ZRZ*).

Snow 1931, Miyoshi et al. 2004, Kawakatsu et al. 2006, Wang et al. 2008, Lee et al. 2009). In agreement with this, a subset of factors that have been shown to affect leaf initiation rate are expressed in developing leaves, consistent with a non-autonomous effect. Possibly, ZRZ is involved in generating a gradient of a signaling molecule, which in turn is interpreted to regulate the time of initiation. Ectopic ZRZ overexpression may disrupt the gradient, and the outcome would depend on the specific timing and location of expression. Testing of this hypothesis will require identification of the ZRZ substrates. The

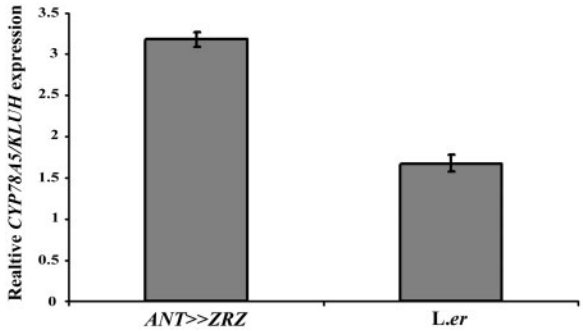

Fig. 6 *ZRZ* overexpression alters the expression of *CYP78A5/KLUH*. Relative expression of *CYP78A5/KLUH* in 21-day-old plants. Relative expression was essayed by qRT–PCR. Shown are averages ± SE ($n = 3$ biological repeats in *ANT>>ZRZ* and $n = 4$ in L.*er*).

involvement of a glutamate carboxypeptidase (Helliwell et al. 2001) and a cytochrome P450 (Miyoshi et al. 2004) in the control of the organ initiation rate supports the involvement of such a signaling molecule in the process. The up-regulation of *CYP78A5/KLUH* gene expression in *ANT>>ZRZ* and *amp1* genotypes, which both produce leaves faster than the wild type, is intriguing as loss of *CYP78A5/ KLUH* function causes a similar phenotype of increased leaf initiation. This may suggest that the timing of leaf initiation responds to the relative spatial and temporal activity of CYP78A5/KLUH rather than to its absolute activity.

An alternative hypothesis might be that the activity of ZRZ is related to the cell energetic balance. The fact that ZRZ overexpression resulted in reduced labeling of mitochondria suggests an impact of ZRZ on the mitochondrion (**Supplementary Fig. S2**). Such an impact could result from direct activity of ZRZ in the mitochondrion or from indirect activity of ZRZ in an adjacent, biochemically related organelle of a similar size (e.g. the peroxisome). The simplest direct scenarios are: (i) ZRZ transporter activity in the mitochondrial membrane exports the MitoTracker dye molecules; or (ii) ZRZ exports other (possibly) charged molecules. In the first scenario, the low probe intensity could be explained by its reduced concentration and in the second scenario its low intensity could result from a decrease in the mitochondrial membrane potential or other essential elements, reducing the activity/vitality of the mitochondrion and thus preventing the fluorescent activity of the MitoTracer dye (Poot et al. 1996).

Elegant models have been proposed recently to explain the involvement of auxin in specifying the site of lateral organ initiation from the SAM (Reinhardt et al. 2003, de Reuille et al. 2006, Jonsson et al. 2006, Smith et al. 2006). However, these models suggest that additional factors control the competence to respond to auxin, as well as the size of the central zone of the SAM, which in turn affects the type of phylotaxis (Giulini et al. 2004) and the rate of organ initiation (Miyoshi et al. 2004, Kawakatsu et al. 2006). ZRZ may be involved in a complex network of communication among different regions of the SAM and its flanks that contribute to the specification of these features.

Materials and Methods

Plant material and genetics

Arabidopsis thaliana plants were grown under long-day conditions (16 h light, 21°C). Arabidopsis transgenic lines were generated by the floral dip method (Clough and Bent 1998). Positive transformants were selected in soil by spraying with BASTA (0.5 mM, 2–3 times). The T-DNA insertion in *zrz-1* plants (Salk 064288) was confirmed by PCR with the Zf14_sk_L primer from the *ZRZ* promoter and the LBa1 primer from the T-DNA. To identify a homozygote line, PCR was performed on 10 progeny. qRT–PCR was performed on mRNA from homozygous seedlings.

The *ANT>>ZRZ* and *STM>>ZRZ* genotypes were produced using the LhG4 transactivation system (Moore et al. 1998). This system comprises driver lines that express the synthetic transcription factor LhG4 under the control of a specific promoter (*PRO:LhG4*), and responder lines, in which a gene of interest is expressed under the control of several copies of the *Escherichia coli* operator (OP), which is recognized by LhG4 (*OP:GENE*). A cross between a driver line and the *OP:ZRZ* responder line resulted in the expression of *ZRZ* under the control of the specific promoter. For example, *ANT>>ZRZ* plants express ZRZ under the control of the *AINTEGUMENTA* promoter, by crossing *ANT:LhG4* and *OP:ZRZ* plants. The *ANT* and *STM* driver lines were kindly provided by Yuval Eshed (Weizmann Institute of Science, Israel).

Plasmids, clones and RNA analysis

The 1015 line was isolated from an enhancer trap population produced with the Ac/Ds transposable elements carrying a GUS (β-glucuronidase) reporter, as described (Sundaresan et al. 1995). Excision events, i.e. transpositions and new re-insertions, were selected for and screened for SAM-specific expression. The insertion flanking regions were isolated by inverse PCR (Mathur et al. 1998). To generate *OP:ZRZ*, the *ZRZ* coding sequence, kindly provided by Dr. Atsushi Kato (Kato et al. 1999), was cloned downstream of an OP array and transferred into the binary pMLBART vector (Gleave 1992). The pART7 vector (Gleave 1992) was used to express the *ZRZ* coding sequence directly under control of the 35S cauliflower mosaic virus (CaMV) promoter. To generate *35S:GFP-ZRZ*, the ZRZ coding region was amplified and cloned into the pSAT6 EGFP C1 vector (Tzfira et al. 2005). Primers used in this study are shown in **Fig. 1** and **Supplementary Table S1**.

RNA isolation and qRT–PCR were done as described previously (Shani et al. 2009).

Light microscopy, GUS staining and sectioning

GUS staining was performed as described previously (Ori et al. 2000). Plants of line 1015 were stained for 2 h. Stained plants

were photographed in 50% glycerol. For sectioning, plants were prepared and sectioned as described previously (Pekker et al. 2005) except that FAA (3.7% formaldehyde, 5% acetic acid, 50% ethanol) was used as fixative.

Transient expression and subcellular localization of ZRZ in Arabidopsis protoplasts

Protoplasts were isolated from Arabidopsis leaf mesophyll and the chimera GFP–ZRZ was transiently expressed using the polyethylene glycol (PEG) transformation method (Locatelli et al. 2003). Protoplasts transiently expressing cytosolic GFP were used as a control. For mitochondrial labeling, the protoplasts were incubated with 100 nM MitoTracker (MitoTracker Red CMXRos M-7512; Invitrogen) according to the manufacturer's protocol. Imaging of GFP and MitoTracker was performed using a fully motorized epifluorescence inverted microscope (Olympus-IX8 Cell-R; Olympus) with the following features: objective lens, plan apochromat, ×60, oil immersion and a numerical aperture of 1.42. The CCD camera used was a 12-bit Orca-AG (Hamamatsu). The filter sets were GFP-3035B-000 and TXRED-4040B, with a zero pixel shift (Semrock). All images were processed using Olympus imaging software Cell-R for Windows.

Quantification of the MitoTracker signal relative intensity in protoplasts

The intensity levels of GFP and MitoTracker were quantified from whole protoplasts using the Olympus Cell-R 3D intensity profile; each cell was optically Z-sliced to 0.28 µm height slices. The mean signal intensity was calculated for each cell separately as the means of the slice intensities. The relative signal intensity of MitoTracker in GFP-expressing cells (ZRZ fused or free GFP) was determined as the ratio of the Mitotracker signal intensity in a GFP-expressing cell divided by the MitoTracker signal intensity in a non-expressing cell (GFP-expressing cell/non-expressing cell). Analysis was always performed on two adjacent cells, one with high expression of GFP and a second cell with no expression.

Supplementary data

Supplementary data are available at PCP online.

Funding

This work was supported by the Israel Science Foundation [grants No. 689/05 and 60/10 to N.O., 953/07 to M.M.].

Acknowledgements

We wish to thank the Nottingham Arabidopsis Stock Center (NASC) for mutant seeds, A. Kato (Hokkaido University, Japan) for the *ZRZ* cDNA, Yuval Eshed for driver lines, and Zach Adam, Alon Samach, David Weiss and members of our laboratories for fruitful discussions and criticism.

References

Anastasiou, E., Kenz, S., Gerstung, M., MacLean, D., Timmer, J., Fleck, C. et al. (2007) Control of plant organ size by KLUH/CYP78A5-dependent intercellular signaling. *Dev. Cell* 13: 843–856.

Barton, M.K. (2010) Twenty years on: the inner workings of the shoot apical meristem, a developmental dynamo. *Dev. Biol.* 341: 95–113.

Bowman, J.L. and Eshed, Y. (2000) Formation and maintenance of the shoot apical meristem. *Trends Plant Sci.* 5: 110–115.

Brown, M.H., Paulsen, I.T. and Skurray, R.A. (1999) The multidrug efflux protein NorM is a prototype of a new family of transporters. *Mol. Microbiol.* 31: 394–395.

Carles, C.C. and Fletcher, J.C. (2003) Shoot apical meristem maintenance: the art of a dynamic balance. *Trends Plant Sci.* 8: 394–401.

Chaudhury, A.M., Lethham, S., Craig, S. and Dennis, E.S. (1993) *amp1*—a mutant with high cytokinin levels and altered embryonic pattern, faster vegetative growth, constitutive photomorphogenesis and precocious flowering. *Plant J.* 4: 907–916.

Clough, S.J. and Bent, A.F. (1998) Floral dip: a simplified method for Agrobacterium-mediated transformation of Arabidopsis thaliana. *Plant J.* 16: 735–743.

Conway, L.J. and Poethig, R.S. (1997) Mutations of Arabidopsis thaliana that transform leaves into cotyledons. *Proc. Natl Acad. Sci. USA* 94: 10209–10214.

Debeaujon, I., Peeters, A.J., Leon-Kloosterziel, K.M. and Koornneef, M. (2001) The TRANSPARENT TESTA12 gene of Arabidopsis encodes a multidrug secondary transporter-like protein required for flavonoid sequestration in vacuoles of the seed coat endothelium. *Plant Cell* 13: 853–871.

de Reuille, P.B., Bohn-Courseau, I., Ljung, K., Morin, H., Carraro, N., Godin, C. et al. (2006) Computer simulations reveal properties of the cell–cell signaling network at the shoot apex in Arabidopsis. *Proc. Natl Acad. Sci. USA* 103: 1627–1632.

Diener, A.C., Gaxiola, R.A. and Fink, G.R. (2001) Arabidopsis ALF5, a multidrug efflux transporter gene family member, confers resistance to toxins. *Plant Cell* 13: 1625–1638.

Durrett, T.P., Gassmann, W. and Rogers, E.E. (2007) The FRD3-mediated efflux of citrate into the root vasculature is necessary for efficient iron translocation. *Plant Physiol.* 144: 197–205.

Elliott, R.C., Betzner, A.S., Huttner, E., Oakes, M.P., Tucker, W.Q., Gerentes, D. et al. (1996) AINTEGUMENTA, an APETALA2-like gene of Arabidopsis with pleiotropic roles in ovule development and floral organ growth. *Plant Cell* 8: 155–168.

Giulini, A., Wang, J. and Jackson, D. (2004) Control of phyllotaxy by the cytokinin-inducible response regulator homologue ABPHYL1. *Nature* 430: 1031–1034.

Gleave, A.P. (1992) A versatile binary vector system with a T-DNA organisational structure conducive to efficient integration of cloned DNA into the plant genome. *Plant Mol. Biol.* 20: 1203–1207.

Gomez, C., Terrier, N., Torregrosa, L., Vialet, S., Fournier-Level, A., Verries, C. et al. (2009) Grapevine MATE-type proteins act as vacuolar H^+-dependent acylated anthocyanin transporters. *Plant Physiol.* 150: 402–415.

Helliwell, C.A., Chin-Atkins, A.N., Wilson, I.W., Chapple, R., Dennis, E.S. and Chaudhury, A. (2001) The Arabidopsis AMP1 gene encodes a putative glutamate carboxypeptidase. *Plant Cell* 13: 2115–2125.

Hou, Y., von Arnim, A.G. and Deng, X.W. (1993) A new class of Arabidopsis constitutive photomorphogenic genes involved in regulating cotyledon development. *Plant Cell* 5: 329–339.

Hvorup, R.N., Winnen, B., Chang, A.B., Jiang, Y., Zhou, X.F. and Saier, M.H. Jr. (2003) The multidrug/oligosaccharidyl-lipid/polysaccharide (MOP) exporter superfamily. *Eur. J. Biochem.* 270: 799–813.

Jonsson, H., Heisler, M.G., Shapiro, B.E., Meyerowitz, E.M. and Mjolsness, E. (2006) An auxin-driven polarized transport model for phyllotaxis. *Proc. Natl Acad. Sci. USA* 103: 1633–1638.

Kato, A., Suzuki, M., Kuwahara, A., Ooe, H., Higano-Inaba, K. and Komeda, Y. (1999) Isolation and analysis of cDNA within a 300 kb Arabidopsis thaliana genomic region located around the 100 map unit of chromosome 1. *Gene* 239: 309–316.

Kawakatsu, T., Itoh, J., Miyoshi, K., Kurata, N., Alvarez, N., Veit, B. et al. (2006) PLASTOCHRON2 regulates leaf initiation and maturation in rice. *Plant Cell* 18: 612–625.

Lee, B., Yu, S. and Jackson, D. (2009) Control of plant architecture: the role of phyllotaxy and plastochron. *J. Plant Biol.* 52: 277–282.

Li, L., He, Z., Pandey, G.K., Tsuchiya, T. and Luan, S. (2002) Functional cloning and characterization of a plant efflux carrier for multidrug and heavy metal detoxification. *J. Biol. Chem.* 277: 5360–5368.

Liu, J., Magalhaes, J.V., Shaff, J. and Kochian, L.V. (2009) Aluminum-activated citrate and malate transporters from the MATE and ALMT families function independently to confer Arabidopsis aluminum tolerance. *Plant J.* 57: 389–399.

Locatelli, F., Vannini, C., Magnani, E., Coraggio, I. and Bracale, M. (2003) Efficiency of transient transformation in tobacco protoplasts is independent of plasmid amount. *Plant Cell Rep.* 21: 865–871.

Magalhaes, J.V., Liu, J., Guimaraes, C.T., Lana, U.G., Alves, V.M., Wang, Y.H. et al. (2007) A gene in the multidrug and toxic compound extrusion (MATE) family confers aluminum tolerance in sorghum. *Nat. Genet.* 39: 1156–1161.

Marinova, K., Pourcel, L., Weder, B., Schwarz, M., Barron, D., Routaboul, J.M. et al. (2007) The Arabidopsis MATE transporter TT12 acts as a vacuolar flavonoid/H^+-antiporter active in proanthocyanidin-accumulating cells of the seed coat. *Plant Cell* 19: 2023–2038.

Maron, L.G., Pineros, M.A., Guimaraes, C.T., Magalhaes, J.V., Pleiman, J.K., Mao, C. et al. (2010) Two functionally distinct members of the MATE (multi-drug and toxic compound extrusion) family of transporters potentially underlie two major aluminum tolerance QTLs in maize. *Plant J.* 61: 728–740.

Mathews, H., Clendennen, S.K., Caldwell, C.G., Liu, X.L., Connors, K., Matheis, N. et al. (2003) Activation tagging in tomato identifies a transcriptional regulator of anthocyanin biosynthesis, modification, and transport. *Plant Cell* 15: 1689–1703.

Mathur, J., Szabados, L., Schaefer, S., Grunenberg, B., Lossow, A., Jonas-Straube, E. et al. (1998) Gene identification with sequenced T-DNA tags generated by transformation of Arabidopsis cell suspension. *Plant J.* 13: 707–716.

McSteen, P. and Leyser, O. (2005) Shoot branching. *Annu. Rev. Plant Biol.* 56: 353–374.

Miyoshi, K., Ahn, B.O., Kawakatsu, T., Ito, Y., Itoh, J., Nagato, Y. et al. (2004) PLASTOCHRON1, a timekeeper of leaf initiation in rice, encodes cytochrome P450. *Proc. Natl Acad. Sci. USA* 101: 875–880.

Moore, I., Galweiler, L., Grosskopf, D., Schell, J. and Palme, K. (1998) A transcription activation system for regulated gene expression in transgenic plants. *Proc. Natl Acad. Sci. USA* 95: 376–381.

Mordhorst, A.P., Voerman, K.J., Hartog, M.V., Meijer, E.A., van Went, J., Koornneef, M. et al. (1998) Somatic embryogenesis in Arabidopsis thaliana is facilitated by mutations in genes repressing meristematic cell divisions. *Genetics* 149: 549–563.

Nawrath, C., Heck, S., Parinthawong, N. and Metraux, J.P. (2002) EDS5, an essential component of salicylic acid-dependent signaling for disease resistance in Arabidopsis, is a member of the MATE transporter family. *Plant Cell* 14: 275–286.

Omote, H., Hiasa, M., Matsumoto, T., Otsuka, M. and Moriyama, Y. (2006) The MATE proteins as fundamental transporters of metabolic and xenobiotic organic cations. *Trends Pharmacol. Sci.* 27: 587–593.

Ori, N., Eshed, Y., Chuck, G., Bowman, J.L. and Hake, S. (2000) Mechanisms that control knox gene expression in the Arabidopsis shoot. *Development* 127: 5523–5532.

Pekker, I., Alvarez, J.P. and Eshed, Y. (2005) Auxin response factors mediate Arabidopsis organ asymmetry via modulation of KANADI activity. *Plant Cell* 17: 2899–2910.

Poot, M., Zhang, Y.Z., Kramer, J.A., Wells, K.S., Jones, L.J., Hanzel, D.K. et al. (1996) Analysis of mitochondrial morphology and function with novel fixable fluorescent stains. *J. Histochem. Cytochem.* 44: 1363–1372.

Reinhardt, D. and Kuhlemeier, C. (2002) Plant architecture. *EMBO Rep.* 3: 846–851.

Reinhardt, D., Pesce, E.R., Stieger, P., Mandel, T., Baltensperger, K., Bennett, M. et al. (2003) Regulation of phyllotaxis by polar auxin transport. *Nature* 426: 255–260.

Rogers, E.E. and Guerinot, M.L. (2002) FRD3, a member of the multidrug and toxin efflux family, controls iron deficiency responses in Arabidopsis. *Plant Cell* 14: 1787–1799.

Sachs, T. (2004) Self-organization of tree form: a model for complex social systems. *J. Theor. Biol.* 230: 197–202.

Saibo, N.J., Vriezen, W.H., De Grauwe, L., Azmi, A., Prinsen, E. and Van Der Straeten, D. (2006) A comparative analysis of the Arabidopsis mutant amp1-1 and a novel weak amp1 allele reveals new functions of the AMP1 protein. *Planta* 225: 831–842.

Schoof, H., Lenhard, M., Haecker, A., Mayer, K.F., Jurgens, G. and Laux, T. (2000) The stem cell population of Arabidopsis shoot meristems in maintained by a regulatory loop between the CLAVATA and WUSCHEL genes. *Cell* 100: 635–644.

Schwarz, S., Grande, A.V., Bujdoso, N., Saedler, H. and Huijser, P. (2008) The microRNA regulated SBP-box genes SPL9 and SPL15 control shoot maturation in Arabidopsis. *Plant Mol. Biol.* 67: 183–195.

Shani, E., Burko, Y., Ben-Yaakov, L., Berger, Y., Amsellem, Z., Goldshmidt, A. et al. (2009) Stage-specific regulation of Solanum lycopersicum leaf maturation by class 1 KNOTTED1-LIKE HOMEOBOX proteins. *Plant Cell* 21: 3078–3092.

Smith, R.S., Guyomarc'h, S., Mandel, T., Reinhardt, D., Kuhlemeier, C. and Prusinkiewicz, P. (2006) A plausible model of phyllotaxis. *Proc. Natl Acad. Sci. USA* 103: 1301–1306.

Snow, M. and Snow, R. (1931) Experiments on phyllotaxis. I. The effect of isolating a primordium. *Philos. Trans. R. Soc. B: Biol. Sci.* 221: 1–43.

Sundaresan, V., Springer, P., Volpe, T., Haward, S., Jones, J.D., Dean, C. et al. (1995) Patterns of gene action in plant development revealed by enhancer trap and gene trap transposable elements. *Genes Dev.* 9: 1797–1810.

Tantikanjana, T., Yong, J.W., Letham, D.S., Griffith, M., Hussain, M., Ljung, K. et al. (2001) Control of axillary bud initiation and shoot architecture in Arabidopsis through the SUPERSHOOT gene. *Genes Dev.* 15: 1577–1588.

Tzfira, T., Tian, G.W., Lacroix, B., Vyas, S., Li, J., Leitner-Dagan, Y. et al. (2005) pSAT vectors: a modular series of plasmids for autofluorescent protein tagging and expression of multiple genes in plants. *Plant Mol. Biol.* 57: 503–516.

Veit, B. (2006) Stem cell signalling networks in plants. *Plant Mol. Biol.* 60: 793–810.

Veit, B., Briggs, S.P., Schmidt, R.J., Yanofsky, M.F. and Hake, S. (1998) Regulation of leaf initiation by the terminal ear 1 gene of maize. *Nature* 393: 166–168.

Wang, J.W., Schwab, R., Czech, B., Mica, E. and Weigel, D. (2008) Dual effects of miR156-targeted SPL genes and CYP78A5/KLUH on plastochron length and organ size in Arabidopsis thaliana. *Plant Cell* 20: 1231–1243.

Winter, D., Vinegar, B., Nahal, H., Ammar, R., Wilson, G.V. and Provart, N.J. (2007) An 'Electronic Fluorescent Pictograph' browser for exploring and analyzing large-scale biological data sets. *PLoS One* 2: e718.

Zhao, J. and Dixon, R.A. (2009) MATE transporters facilitate vacuolar uptake of epicatechin 3′-O-glucoside for proanthocyanidin biosynthesis in Medicago truncatula and Arabidopsis. *Plant Cell* 21: 2323–2340.

Zondlo, S.C. and Irish, V.F. (1999) CYP78A5 encodes a cytochrome P450 that marks the shoot apical meristem boundary in Arabidopsis. *Plant J.* 19: 259–268.